

MASTE.

MATERIALS COMPATIBILITY IN LIQUID SODIUM

290 6800

W. F. Brehm
Hanford Engineering Development Laboratory
Richland, Washington 99352

NOTICE
This report was prepared as an account of work sponsored by the United States Government. Neither the United States nor the United States Department of Energy, nor any of their employees, nor any of their contractors, subcontractors, or their employees, makes any warranty, express or implied, or assumes any legal liability or responsibility for the accuracy, completeness or usefulness of any information, apparatus, product or process disclosed, or represents that its use would not infringe privately owned rights.

August 1978

For Presentation at the NACE South Central Regional Conference in Denver, Colorado, October 3, 1978.

By acceptance of this article, the Publisher and/or recipient acknowledges the U. S. Government's right to retain a nonexclusive, royalty-free license in and to any copyright covering this paper.

DISTRIBUTION STATEMENT A UNCLASSIFIED

SP

DISCLAIMER

This report was prepared as an account of work sponsored by an agency of the United States Government. Neither the United States Government nor any agency thereof, nor any of their employees, makes any warranty, express or implied, or assumes any legal liability or responsibility for the accuracy, completeness, or usefulness of any information, apparatus, product, or process disclosed, or represents that its use would not infringe privately owned rights. Reference herein to any specific commercial product, process, or service by trade name, trademark, manufacturer, or otherwise does not necessarily constitute or imply its endorsement, recommendation, or favoring by the United States Government or any agency thereof. The views and opinions of authors expressed herein do not necessarily state or reflect those of the United States Government or any agency thereof.

DISCLAIMER

Portions of this document may be illegible in electronic image products. Images are produced from the best available original document.

MATERIALS COMPATIBILITY IN LIQUID SODIUM

W. F. Brehm

Hanford Engineering Development Laboratory

Richland, Washington, 99352

Presented at NACE South Central Regional Conference

Denver, Colorado

October 1978

One of the uses of liquid sodium metal is as coolant for nuclear power reactors. Sodium is chosen because (1) it has good heat transfer properties at low pressure, (2) it does not degrade a fast neutron spectrum, (3) it is relatively inexpensive and readily available, and (4) it is compatible with reactor materials at temperatures of interest. Sodium-cooled reactors have operated successfully for the past twenty years, including experience in the United States, Western Europe, the Soviet Union, and Japan.

Most of the development work with material compatibility in liquid sodium has been in support of reactor design and operation. Extensive experimental studies have been completed to establish the types and rates of reaction of sodium with reactor materials; key results will be discussed in the paper.

In summary, the austenitic stainless steels used for primary containment and fuel cladding materials meet the requirements for reactor service, including compatibility with the liquid sodium, at temperatures up to 750°C; however, sodium interaction with materials must be factored into reactor design and operation for components with service temperatures above 400°C (this includes essentially all major components and piping in the heat transport system.) Specialty materials such as hardfacing alloys are also required for certain applications. Improved materials are being developed for future use.

Mass loss rates of austenitic stainless steels in sodium are quite modest, equivalent to above 25 μm per year at 700°C and 1 μm per year at 550°C. This rate must, however, be factored into design and performance criteria for thin-walled fuel cladding. Nonuniform corrosion, possibility of intergranular attack in some materials, possible gain or loss of carbon and nitrogen, and deposition of dissimilar metals on surfaces can affect the properties of materials during service. Therefore, a simple corrosion or waste allowance is not sufficient when assessing environmental effects for reactor components.

Thorough understanding of sodium-material interaction is needed to answer these specific questions:

- 1) The fuel cladding is only 0.20 to 0.40 mm thick, yet is subject to temperatures up to 700⁰C and biaxial stresses of 70 MPa (10,000 psi). What is the wall-thinning rate in the high velocity (6 meters/sec) sodium stream? Is there intergranular penetration? Does selective leaching of elements change the strength, ductility, or swelling resistance of the cladding?
- 2) Are interstitial elements carbon, nitrogen, and boron transported from one place in the sodium circuit to another, and what effect does interstitial transport have upon the properties of donor and receiver material?
- 3) Does deposited mass-transfer material degrade heat transfer in heat exchangers, or does it change the surface roughness such that pressure drops and/or flow distributions are altered?
- 4) Material removed by mass transfer from the reactor core is highly radioactive. Will deposition of this radioactive material create maintenance problems from high radiation exposures to workers?
- 5) Are all component specialty materials known to be compatible with sodium?
- 6) The structural materials in a reactor operate at lower temperatures (up to about 575⁰C) and have larger cross-section, but have

service lifetimes up to 30 years. Are the mass transfer processes and effects on properties understood well enough to extrapolate data to 30 year lifetimes?

A schematic of a sodium-cooled reactor and the areas of interest is shown in Figure 1.

SUMMARY

Significant progress have been made in the last decade, both in understanding the process of material behavior in experimental sodium systems and in evaluating materials performance from actual reactor operations.

In general, enough data have been generated under well-controlled conditions to make reasonably accurate and confident predictions of corrosion behavior for steel in sodium even though the theory has not completely been developed. Deposition phenomena are not so well defined, at least with respect to establishing quantitative correlations.

Radioactive mass transport has perhaps been more closely characterized, because the measurement of

the movement of radioactive species may be determined more precisely. The deposition of radioactive corrosion products in out-of-core components may limit accessibility for maintenance; however; promising methods for preventing radioactive mass transport to maintenance zones have been demonstrated in the laboratory. Satisfactory materials for hard-facing and low-friction applications in sodium have been found.

The importance of maintaining the purity of the coolant sodium has been demonstrated repeatedly. Impurity meters for real-time indication of oxygen and hydrogen levels have been developed for test facilities. Instruments for measuring carbon in sodium are in laboratory development. Cleaning processes for the removal of sodium without corrosion or metallurgical damage to the substrate metal have been developed and demonstrated. The previous statements do not mean that all materials compatibility problems have been solved; improved materials for reactor service; considering many other factors beside sodium compatibility, are being developed. Their interaction with sodium must be characterized and understood; ongoing test programs are accomplishing this.

EXPERIMENTAL TECHNIQUES

Because of the reactive nature of sodium, and the effect of small amounts of impurities on materials compatibility, it is necessary to provide protection from atmosphere and moisture contamination. When suitable precautions are taken and sufficient monitoring instrumentation is provided,

flowing sodium systems can be maintained within close operating tolerances.^(1,2)

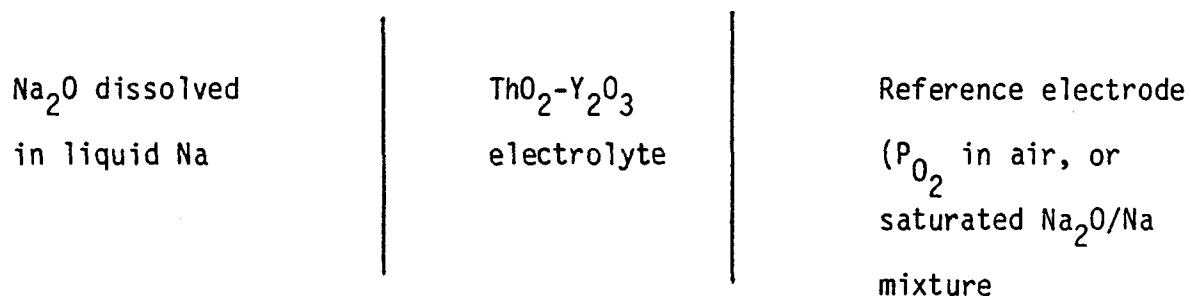
Most experiments are done in a "sodium loop," such as the one shown schematically in Figure 2. Provisions are made for insertion and withdrawal of specimens into inert gas locks to protect surfaces from atmospheric contamination if necessary, and for purification of sodium by cold-trapping and/or hot-trapping,* and an inert cover gas, usually argon or helium, over the sodium. Even though sodium flowrates and pipes sizes in reactors are quite large, the spacing between fuel pins is only 1.0 to 1.5 mm. For this reason, it is possible in properly designed tests to duplicate the temperature, velocity, and Reynolds number of conditions at the fuel pin cladding/sodium interface. It is also possible, at additional effort and expense, to duplicate the steep axial temperature gradient characteristic of a reactor core to determine the effect of temperature profile on interaction behavior. When such evaluation is being done, the regenerative heat exchanger of Figure 2 is replaced with larger heater and cooling sections.

A key step in analyzing mass transfer interactions was the development of the vanadium-wire equilibration technique⁽³⁾ as a standard method for analyzing oxygen content of sodium. This method brings sodium and vanadium

*A cold trap removes oxygen, hydrogen, and carbon impurity species from sodium by cooling the sodium stream to controlled temperatures where the species become insoluble, and providing nucleation sites for the various oxides, hydrides, etc. A hot trap removes impurities by contacting sodium with hot (600°C or above) zirconium, titanium, or other reactive metals. The impurities react with the hot reactive metal and diffuse into it.

into equilibrium at constant controlled temperature. The vanadium is then analyzed for oxygen by vacuum-fusion analysis, and thermodynamic partition information is used to back-calculate the oxygen level of the sodium. It is important to note that the method is self-consistent as long as the equilibrium temperature is maintained constant and the vacuum fusion analysis is standardized. Both those requirements are easily fulfilled in practice. In this paper, all oxygen levels quoted are those derived from vanadium wire analysis.

An in-line meter has been developed which measures oxygen activity in sodium by electrochemical means.⁽⁴⁾ A $\text{ThO}_2\text{-Y}_2\text{O}_3$ solid electrolyte is immersed in the sodium, establishing a cell:



Since each electrolyte tube varies slightly in its output voltage, the vanadium wire analysis is used for absolute calibration of the oxygen meter, whose output voltage is then continuously monitored.

Hydrogen (and its isotopes deuterium and tritium) is reliably measured in sodium by means of a nickel diffusion tube which connects to a high vacuum system. The hydrogen in the sodium is in equilibrium with hydrogen

gas in the vacuum system by diffusing through a nickel membrane. An absolute measure of the hydrogen level is obtained by evacuating the vacuum system and then measuring the hydrogen pressure after equilibration. A dynamic reading may be taken by reading the ion pump current during steady state evacuation. An equilibration method for hydrogen, using a thin foil of metallic scandium which is equilibrated by immersion in the sodium and subsequently removed for analysis, is also used.

Carbon measurement in sodium by means of meters and equilibration procedures is not as well developed. Nevertheless, such devices for monitoring the carbon activity in sodium are being developed in the U.S. and abroad. The carbon meter uses a metal membrane through which carbon will diffuse. The carbon is reacted on the non-sodium side of the membrane to form carbon monoxide, which is then swept out and measured in an external system. Equilibration methods use tabs of iron or special alloys which are then removed from the sodium for analysis, similar to the vanadium-wire technique for oxygen determination.

Since the interaction of sodium with materials is complicated and cannot be described simply in terms of weight loss or uniform corrosion, additional evaluation methods are required.

Typical methods of determining mass transfer behavior at both mass loss and deposition sites include light metallography, electron microscope analysis of topography and surface concentration, incremental analysis of

sequential layers of material adjacent to the specimen surfaces, and electron microprobe examinations. Auger electron spectroscopy, glow-discharge optical spectroscopy, and ion-bombardment because of their sensitivity and ability to analyze extremely small samples, are becoming useful analytical tools. Chemical analysis of sodium is sometimes performed, but has not been particularly useful in analyzing mass transfer behavior because of sampling difficulties and inconsistent data on the solubility of structural materials in sodium. When radioactive materials are used in experiments, standard radiochemical analysis in combination with sequential incremental analysis and weight less measurements can be used to establish radionuclide source rates. Gamma spectrometry of test loops and actual reactor piping has been completed, as well as similar evaluation of test specimens and reactor components removed from service. Radiochemical analysis of reactor and test loop sodium is also performed, again with inconsistent results.

Results of metallographic, microscopic, and sequential analysis of surfaces of sodium-exposed material are shown in Figures 3 through 6.

SODIUM-MATERIAL INTERACTION PHENOMENA

Austenitic Stainless Steel - Because of the large amounts of austenitic stainless steel used in the reactors; most of the experimental investigations have concentrated on this material. This section describes mass transfer behavior of austenitic stainless steel in the hot leg or maximum temperature region of a test loop or reactor with a system temperature gradient (ΔT)

of 30⁰C or more. In general, measurable mass loss is observed at temperatures above 400⁰C; preferential loss of nickel causes surface and grain boundary transformation to ferrite above about 600⁰C.

In an austenitic stainless steel, the mass loss is not uniform with time. In general, the constituents of the steel that are thermodynamically favored to be associated with the sodium (such as nickel and chromium) are leached out, resulting in the altered surface mentioned above. The leaching process is fed by solid-state diffusion from the interior of the specimen. After a time, the diffusion flux of the species decreases to that equivalent to uniform recession of the surface. A steady state is eventually reached where the mass loss rates become stoichiometric and time-variant. Note that the corroding surface is now considerably enriched in iron, enough to transform it to ferrite. It has been reported that exposure longer than 10,000 hours is required at 700⁰C to obtain time-invariant mass loss rates. Growth of the surface ferrite layer (proportional to square root of time) has been reported to continue past 500 hours at 700⁰C.⁽⁵⁾ The times for attainment of steady state are even longer at lower temperatures. Breeder reactor fuel elements have projected service lifetimes of 8000 to 25,000 hours, almost always at temperatures below 700⁰C so the steady mass loss rate is not likely to be attained in many fuel elements. Reactor plant components with service lifetimes up to 30 years are more likely to attain time-invariant mass loss rates. However, many of them are in the decreasing temperature or cold leg region and will experience mass gain or deposition.

Velocity Effects - The mass loss rate increases with fluid velocity up to a certain value, then levels off. The reason given for this phenomenon is that up to a certain velocity, the mass loss is dependent on events such as diffusion of metallic species and oxygen to and from the metal surface through hydrodynamic boundary layers.^(5,6,7) Above a limiting value, other processes such as surface oxidation, surface bond breaking, and solid-state diffusion become the slow step in the mass loss process. This effect is shown schematically in Figure 7. Obviously, the plateau is a function of hydrodynamic boundary layer thickness, and the plateau velocity will be dependent on temperature, geometry, and perhaps oxygen content of the sodium. Two rule-of-thumb figures are mentioned for the velocity-dependent limit, a velocity of 4.6 m/s (15 ft/sec) and/or a Reynolds number of 5×10^4 . Note that fuel cladding assemblies fall in the velocity-independent regime. Hydrodynamic theory predicts mass loss to vary with the the 0.8 power of velocity within the velocity-dependent range; results are not noticeably different. An analysis of hydrodynamic parameters and their relation to the effect of sodium velocity on mass loss rates have been published.⁽⁸⁾

Preferential Leaching and Oxygen Effects - In the relatively complex austenitic stainless steel alloys, the mass loss appears to occur by two competing processes: oxidation of the surface and dissolution of the oxide phase into the sodium, and direct dissolution of alloy constituents into sodium. Some alloy constituents always dissolve directly into sodium at a faster rate than the surface is removed by the oxidation process. At typical low oxygen activities found in loops, chromium, nickel, manganese, and

silicon initially migrate out faster than the surface recedes. Iron is the major element removed by the oxidation process, although the removal of chromium and silicon may also depend on oxygen activity in sodium. Cobalt and molybdenum are preferentially retained, it being favorable for them to be retained within the steel and thus to accumulate at the solid-liquid interface. Whether the preferential retention is due to thermodynamic considerations or to slow dissolution rates of the elements into sodium is not known. The effects of this preferential leaching have been shown in Figures 3 through 6.

A general increase in mass loss rates with oxygen level in sodium has been observed. Weeks and Isaacs' theory⁽⁹⁾ predicts that iron is the only constituent of stainless steel whose mass loss rate depends on oxygen level, and that the mass loss rate of an austenitic stainless steel is proportional to the $2x$ power of oxygen activity, where x is fraction of iron in the alloy. (For example, for 316 stainless steel containing 65% iron, the exponent on oxygen concentration would be 1.3.) Another study by Bagnall and Jacobs⁽⁶⁾ examined mass loss rates of 316 stainless steel and concluded that there was no statistical justification for an exponent other than 1 on oxygen concentration. A study by Brehm et al.,^(10,11) on irradiated 316 stainless steel at 604°C, confirmed the Weeks and Isaacs theory that oxygen level in sodium significantly influenced only the mass loss of iron. In the phase of this study where mass loss was determined at oxygen levels of 2.5 and 0.5 ppm, the decrease in mass loss was only about a factor of two at the lower oxygen level. Decreasing the oxygen level to less than 0.01 ppm with a hot trap purification did not reduce the mass loss rate below that obtained at 0.5 ppm oxygen.

It is probable that at oxygen levels less than 1 ppm, the mass loss during the period before steady-state is attained is dominated by loss of nickel and chromium from the steel, and that variation of iron loss with oxygen is less important in the total mass loss. In addition, the iron loss at the low-oxygen levels attained by hot-trapping mentioned above was not reduced below that at 0.5 ppm. Therefore, mass loss rates of austenitic stainless steels do not appear dependent on oxygen levels below 1 ppm oxygen. Still not clear is the question of why loss of chromium, which forms chromium oxides and sodium chromites supposedly more stable than the corresponding iron compounds, is not more sensitive to oxygen at oxygen levels in the 1 to 10 ppm range. At high oxygen levels (above 10 ppm) the oxides of iron dominate the mass loss process, the interfaces recede more rapidly, and the preferential leaching and ferrite layer formation are not observed.⁽¹²⁾ This case is of limited practical interest since reactors and large test rigs have technical specifications which prohibit operation at such high oxygen levels.

Downstream Effect - In a situation where there is an isothermal section of material with constant fluid dynamics (e.g., constant velocity and no flow perturbations), and the mass loss rate of stainless steel in sodium decreases with length along the isothermal section. This phenomenon is called the downstream effect, and has been seen in every instance where it could be measured. Generally speaking, the higher the upstream or zero-downstream mass loss rate, the more pronounced is the downstream effect, as seen in Figure 8, reproduced from Reference 5. The downstream effect is thought to be caused by

saturation of the sodium stream with alloy constituents, decreasing the driving force for dissolution. Alternately, for an oxidation process, the downstream effect could be caused by depletion of oxygen in the sodium stream. Another explanation, proposed by Weeks and Isaacs is the "poisoning" of active corrosion sites by redeposition of chromium and nickel at the downstream positions.⁽⁹⁾

Temperature-Gradient Effects - In the core of a reactor the high power density causes the sodium temperature to rise as much as 250°C per meter of fuel element channel length. The fuel cladding temperature will be 10 to 15°C hotter than the sodium temperature because of the intense radial heat flux within the fuel cladding. (Because of the high thermal conductivity of sodium and the absence of a distinct oxide layer on the cladding surface, the film delta T or thermal boundary layer is only 10 to 15°C, rather than up to 100°C as in water-cooled reactors.)

Under these conditions, the zero downstream mass loss rate is roughly twice that obtained at otherwise identical conditions. This effect has been confirmed by evaluation of in-reactor fuel cladding⁽¹³⁾ as well as in carefully controlled laboratory tests where special heating sections were built to duplicate the thermal gradient.^(9,14,15) It has been found that duplicating the axial thermal gradient is sufficient to obtain valid results, if the 10 to 15°C film delta T is accounted for by raising the test temperature by that much.

The cause of this increased mass loss rate is the reverse of the "saturation" model downstream effect; that is, the transit time of the sodium past the material is so rapid and the temperature rise is so steep, that the sodium is under-saturated with alloy constituents, increasing the driving force for dissolution. It is worth noting that in one study where this effect was not observed, the oxygen level was higher than in tests where the temperature gradient effect was observed. A possible explanation is that the oxidation controlled mass loss phenomenon is less sensitive to temperature profile (this thus assumes that there is always sufficient oxygen available at higher oxygen levels). Fuel pin wastage allowances have been adjusted to compensate for the accelerated mass loss in a reactor core.

Depleted Zones and Intergranular Penetration - The preferential loss of nickel and chromium from austenitic stainless steel leaves a depleted zone in the remaining material. Part of the depleted zone will transform to ferrite; ferrite layer thicknesses of 15 to 25 μm have been reported after 10,000 hours at 700^oC; the total depleted zone is up to 40 μm deep at those conditions. At far downstream positions, the preferential loss of nickel and chromium is decreased, and as a result, the ferrite layer thickness is also reduced. Ferrite is observed in grain boundaries at temperatures as low as 550^oC, and on the surface at 600^oC.

The faster diffusion rates in grain boundaries can lead to actual intergranular penetration by sodium (actually dissolution of grain-boundary regions). Intergranular penetration in austenitic stainless steel is not

common below 750°C. It is important to note that classic liquid-metal embrittlement,⁽¹⁶⁾ or deep grain boundary attack involving an intermediate liquid phase⁽¹⁷⁾ do not occur with austenitic stainless steel and properly cold-trapped sodium. Occasionally intergranular attack up to 50 micrometers deep is seen in system cold legs; it is possible that this reaction is caused by local very high oxygen concentrations in sodium left in the test system during shutdowns between runs, and subsequent oxidation of localized areas. The resultant high oxygen sodium during system startup causes the intergranular penetration.

Mass Loss Correlations - Several parametric equations for mass loss have been developed;^(6,9,18) the one most generally used in the USA is the "Bagnall-Jacobs" correlation,⁽⁶⁾ given below and in Figure 9.

$$S/\emptyset = 170 \times 10^9 \exp (-18120/T) ,$$

where T = degrees Kelvin

S = corrosion rate, micrometers/year

\emptyset = oxygen level in ppm, given by vanadium wire analysis.

This expression is for velocities above 4.76 m/s.

For high axial thermal gradient conditions, the value of S obtained from the equations should be doubled. For velocities less than 3 m/s, the recommended expression is:

$$S/\phi = 2.97 \times 10^8 + 2.71 \times 10^8 \exp (-18120/T) ,$$

where V = sodium velocity in m/s.

It is the author's opinion that at oxygen levels less than 1 ppm, the value of 1 ppm be used in the mass loss equation because of the oxygen-independent mechanism of mass loss of chromium, nickel, and iron dominating the process at low oxygen levels. Note that the activation energy in the Bagnall-Jacobs correlation is 36.2 Kcal/mol. This value suggests surface reaction rather than fluid boundary layer diffusion as a controlling step in the reaction.

A correlation for equilibrium depth of alloy depletion (not ferrite layer thickness) has been proposed:⁽⁶⁾

$$t = (5.21 \times 10^{15})/S \exp (-29685/T) ,$$

where t = equilibrium thickness, micrometer

S = mass loss rate (micrometer/year).

This equation suggests an activation energy of about 60 Kcal/mol, which is typical of substitutional solid-state diffusion in austenitic steels. This correlation is shown in Figure 10.

Standard mass transfer models based upon hot and cold leg equilibrium solubilities of alloy constituents, plus kinetic rate constants from kinetic theories and fluid dynamics, have not proved useful in describing mass loss behavior of austenitic stainless steels. The complexity of the mass loss process in an eight (minimum) component system (Fe, Cr, Ni, Si, Mo, Mn, Na, O, etc.) and the lack of reliable solubility data hinder this effort.

Effect of Stress and Radiation Environment - No detectable effect of either applied stress or neutron irradiation on mass loss has been observed. The effect of cold work (as in 316SS fuel cladding) is uncertain, small increases in mass loss rate in 20% cold worked 316SS have been reported.⁽¹⁹⁾ Furthermore, significant amounts of fast neutron sputtering of fuel cladding in reactor cores is absent. These factors add to the confidence one is able to have in applying out-of-reactor data to reactor design and operations support.

Effect of Minor Alloy Variations - The mass loss rates among various austenitic stainless steels do not vary significantly, even though small differences in alloy composition of the steels can provide significant differences in strength, ductility, fabricability, resistance to aqueous corrosion, and resistance to radiation damage. The significance of this is that mass loss correlations developed for 316 stainless steel can be used for other austenitic stainless steels, within the limitations described, without significant error.

Interstitial Transport - Interstitial element carbon, nitrogen, and boron can migrate from high activity regions to low activity regions. The activity gradient can be provided by dissimilar metal compositions or temperature gradients within the system. The sodium provides a carrier for the interstitial atoms to move from one part of flowing system to another. With a cold trap operating, carbon (in particular) activity in the sodium is reduced, so that carbon migration from the steels to the sodium is thermodynamically favored under some conditions. Several theoretical and experimental analyses of this situation have been reported in References 20 through 25.

In general, nitrogen and boron are rapidly lost from steels in the hot leg of test systems.^(5,26,27) The nitrogen loss is not of concern because (1) fuel cladding is restricted to 100 ppm nitrogen, leaving little nitrogen to lose, and (2) if carbon content in structural materials is maintained above 400 ppm, code-allowable stress properties are maintained regardless of the nitrogen level. The loss of boron did not seem to affect the long-term creep properties of the German steels in which it was reported⁽²⁷⁾.

Carbon will migrate in or out of an austenitic stainless steel depending on the local activity and the availability of carbon for diffusion. Briefly:

- 1) All unstabilized, annealed austenitic stainless steels will lose carbon above about 550°C. At 650°C and above, because of the rapid diffusion of carbon, an entire 0.38 mm thickness of fuel

cladding can be decarburized to less than 100 ppm carbon in 1000 hours.

- 2) All stabilized steels (Nb, Zr, or Ti additions) will pick up carbon if a mechanism exists to provide it.
- 3) Cold work and irradiation accelerate carbide precipitation of $M_{23}C_6$ carbides in 316 stainless steel. The carbon is no longer free to diffuse, and decarburization does not occur or occurs very slowly at $600^{\circ}C$ and below. In-reactor evaluation of 20% cold-worked cladding has shown no decarburization (and no loss of nitrogen) after 5328 hours at up to $675^{\circ}C$; ⁽¹³⁾ however, an out-of-reactor test on 20% cold-worked, pressurized material showed significant carbon loss after 2000 hours at $650^{\circ}C$. ⁽²⁸⁾
- 4) Depth of carburization in reactor components is likely to be small, 100 micrometers or less, because of the relatively low temperature ($600^{\circ}C$ or less) and the precipitation of $M_{23}C_6$ and M_7C_3 phases near the metal surface.
- 5) The ferritic 2-1/4 Cr - 1 Mo steel favored for steam generators is subject to decarburization because of the low solubility of carbon in ferrite. Because of relatively low temperatures (450 to $575^{\circ}C$), again the process is relatively slow. Use of a stabilizer (Nb, Ti,

or Zr) as an alloying element, or use of a 9% or 12% Cr ferritic steel, will suppress the decarburization for all practical purposes.

SODIUM COMPATIBILITY OF OTHER MATERIALS

Both metallic and nonmetallic materials are used in reactors, generally as part of specialty components such as bearings, load pads, structural materials, etc. The materials have, for the most part, been tested in sodium at or near their expected service conditions. Austenitic high strength steels containing 10% to 43% nickel, rather than the 8% to 14% found in stainless steels, are being tested for future use as fuel cladding and ducts. Sodium compatibility testing of these candidate materials, as well as other materials used for reactor components, has been reported.

The results can be summarized as follows:

- 1) Cobalt-rich alloys and molybdenum alloys have extremely low mass loss rates in sodium up to 700°C. When used in a system constructed principally of austenitic stainless steel, these non-ferrous materials show deposition of iron, chromium, and nickel. Nickel-base materials Alloy 600 and Alloy 718 have extremely high mass loss rates and intergranular penetration in sodium at 600°C and above. (26,29) Alloy 718 is acceptable for reactor components below 600°C, but not for fuel cladding.

- 2) The ferritic alloy steels and carbon steels show about the same mass loss rates as the steady-state loss rates on austenitic alloys. As mentioned, the 2-1/4 Cr - 1 Mo unstabilized steels are subject to decarburization but the rate can be quite slow. Plain carbon steels are subject to very rapid carbon loss because of lack of stabilizing elements such as Cr to reduce carbon activity in steel and because of rapid carbon diffusion rates. They should be used with caution above 400°C in sodium.
- 3) Use of niobium, zirconium, vanadium and tantalum alloys in stainless steel systems is questionable at 500°C and above because of carbon and oxygen absorption and resulting embrittlement. Mo and W-based alloys are suitable.
- 4) The use of Mo-clad tantalum for control rods has been considered. Cobalt and tantalum become extremely radioactive in a neutron flux, thus adding to the radioactivity burden if use in the reactor core and adjacent regions. (It is recognized that there are sometimes no alternatives to cobalt-base bearing alloys.)
- 5) Alloys PE16, 706, and A286 have shown mass loss rates roughly equal to 316 SS at 700°C after 2000 hours.⁽²⁹⁾ Alloy PE16, however, is much more susceptible to intergranular attack than the other alloys. A286 had a significantly smaller diffusion zone than other materials.

- 6) Normally corrosion-resistant metals, such as copper, silver, gold, and platinum, dissolve rapidly in sodium at all temperatures and are not satisfactory for sodium service (an exception is the use of thin layers as sacrificial coatings to facilitate wetting, as in under-sodium ultrasonic viewing devices.) Organic-halide polymers, such as teflon, react violently with liquid sodium even in inert atmospheres.

RADIOACTIVE MASS TRANSPORT

Buildup of radioactive species in primary system piping will occur due to transport of radioactive materials from the reactor core to external piping and components. Reactors with core outlet temperatures near 500°C have experienced significant amounts of radioactive mass transport. It is predicted that reactor operations with core outlet temperatures of 500 to 600°C will produce radiation fields over 1 R/hr in primary system equipment cells. Experience has shown that maintenance operations are difficult in such conditions. The activated corrosion products ^{54}Mn and ^{60}Co , with lesser amounts of ^{58}Co , ^{51}Cr , and ^{59}Fe will be present, as will ^3H (tritium). Fission products ^{137}Cs , $^{140}\text{Ba-La}$, $^{95}\text{Zr-Nb}$ and others will be present if operation with breached fuel cladding is permitted. It is to be noted that cladding mass loss rates equivalent to 5 μm per year, satisfactory from a structural integrity standpoint, generate enough radioactive material to produce high radiation levels in primary equipment cells.

Experiments with radioactive materials were required since existing theories do not treat the mass loss of the minor alloying elements manganese and cobalt from stainless steel. The production of ^{60}Co can be controlled (but not entirely eliminated) by restricting Co content of in-core materials (the Co is an impurity in nickel), but ^{54}Mn is created by a transmutation (n,p) reaction on iron. Experiments at 604°C showed the following:^(10,11,19)

- 1) Decreasing oxygen content from 2.5 to 0.5 ppm decreased ^{54}Mn release about 30% and decreased ^{60}Co release about a factor of 3.
- 2) Almost 10 times as much ^{54}Mn as ^{60}Co was released, because of the preferential leaching of ^{54}Mn and preferential retention of ^{60}Co . The overall reduction in radioactivity release at the lower oxygen level was statistically significant but insufficient to solve the problem.
- 3) Use of a hot trap to produce less than 0.01 ppm oxygen in sodium did not reduce nuclide source rates below those observed at 0.5 ppm oxygen.
- 4) There is some evidence that the apparent effect of oxygen level on ^{60}Co transport is indicative of ^{60}Co being transported as an Fe-Mo-Co rich (90+% iron) particulate species. The Fe release is dependent on oxygen level. Examination of individual specimens shows a correlation between Fe and ^{60}Co release.

- 5) A 12,000 hour nuclide release experiment at 540°C, 0.5 ppm oxygen showed much less preferential retention of ^{60}Co than at 540°C, preferential leaching of ^{54}Mn , and significantly less mass loss. The ^{60}Co and ^{54}Mn release was reduced by factors of 1.6 and 3, respectively, from that at 604°C.⁽³⁴⁾ This reduction in nuclide release is not sufficient to completely solve the problem.

- 6) Control measures based upon selective deposition are being developed.

DEPOSITION

Essentially all of the material removed from mass loss regions in a reactor or test loop is deposited in the circuit; the sodium contains only a few ppm of metallic and non-metallic species, often less. The deposition occurs in far downstream regions of hot legs, in decreasing temperature regions, in cold legs, and under certain conditions, in rising temperature zones. It is believed that slight reductions in sodium stream temperature can cause deposition to occur. Because of the mixing of bypass flow (used to cool the reactor vessel wall) and the flow through the fuel bundles, at the top of the reactor vessel, most of the piping and components of a loop-type reactor will be deposition sites.

There are three reasons for characterizing material deposition:

- (1) Deposition of radioactive species can create handling and maintenance

problems (2) The possibility exists for heat transfer to be degraded by deposited species (3) In some cases, increased pressure drop may occur under certain geometrical and temperature conditions. The discussion below summarizes results to date; it will be apparent that information on deposition is much less quantitative than that for material loss.

Mass transfer deposits in reactors and piping have been examined by most groups that did "corrosion" tests. Deposits were of a variety of chemical forms and morphologies; chief results were as follows:

- 1) Chromium and cobalt tended to deposit near the release site often in regions in the hot leg where definite mass loss of iron and nickel were still occurring.
- 2) Iron tended to deposit uniformly in a test system.
- 3) Nickel, manganese, and silicon deposit in heat exchangers and cold legs.
- 4) Radioactive cesium and iodine migrate toward the lower temperature regions, usually the cold trap. These species have a considerably higher solubility than the structural materials and will remain in solution until they can be precipitated in the cold trap. The cold trap will usually irreversibly remove other species; however,

because of their low solubility, they most often deposit on primary system walls.

- 5) Iron is usually found as alpha iron or iron oxides. It is theorized that ^{60}Co is associated with alpha iron or iron oxide particulates.
- 6) Chromium is usually found as chromium carbide.
- 7) Manganese and nickel are often found together in modules in system cold legs. Mn and Ni are not associated with oxygen. Si deposition is not well characterized.
- 8) The more oxygen in the system, the more oxide in the deposits.
- 9) The higher the temperature and the less the oxygen level, the more adherent the deposits. Metallic species are, in general, more adherent to the deposition substrate than nonmetallic species.
- 10) Deposited radioactive species diffuse into the underlying base metal in the hot leg, as much as 20 micrometers. The ^{54}Mn in cold legs is part of the Ni-Mn rich deposit and is mostly deposited on, rather than diffused into, the metal.⁽³¹⁾

- 11) At temperatures above 400°C, a significant fraction of the deposited corrosion products are tightly adherent or diffused into the base metal. Fission products ^{137}Cs , ^{134}Cs , and ^{131}I are not adherent and can be removed by water or alcohol sodium removal processes. Alkaline earth and refractory metal fission products such as $^{140}\text{Ba-La}$ and $^{95}\text{Zr-Nb}$, as well as (U,Pu) and (U,Th) oxide fuel, probably exist as insoluble oxides; their adherence to surfaces is not well characterized.

- 12) All radioactive and nonradioactive species have shown a tendency for more rapid deposition at increased turbulence, at both hot and cold leg temperatures. This behavior is typical of both atomic and particulate species. Particles can be filtered out of a sodium stream. This merely indicates that the filter was a nucleation site for deposition, rather than providing quantitative information. Particulates, if they exist, are probably smaller than 1 micrometer.

A potential loss of up to 10% of heat exchanger heat transfer capability has been estimated,⁽³²⁾ from deposition on heat exchanger tubes. This possibility must be evaluated because of the impact on plant capital cost if heat exchangers are required to be oversized to accommodate the potential loss of heat transfer.

The loss of flow capacity ("flow-impedance phenomena") is recognized as a phenomenon caused by deposits affecting surface roughness and changing the friction factor. Actual loss of flow from physical narrowing of flow channels would require mass transfer rates at least two orders of magnitude higher than those observed. This effect is under active investigation,^(33,34) available data indicate that a crystalline phase containing sodium and silicon deposits from the flowing liquid upon a small (5° or 10°C) temperature drop.

Selective deposition, i.e., the preferential deposition of one element on another one, is observed. This effect is used to develop "nuclide traps", devices which remove radioactive species from sodium at predetermined locations. The concept has great applicability for removing radionuclides away from primary system components requiring maintenance. For example, pure nickel is very effective at removing ^{54}Mn and ^{60}Co at 500°C and above: above,⁽²⁵⁾ while various forms of graphite rapidly absorb ^{137}Cs and ^{134}Cs in the temperature range $100^{\circ}\text{-}350^{\circ}\text{C}$.⁽³⁶⁾ In-reactor tests of these devices are in progress. See Figures 11 and 12.

EFFECTS ON PROPERTIES

The sodium effects on the material properties of austenitic stainless steel are the sum of (1) wall thinning, (2) ferrite layer, (3) intergranular attack and diffusion zone, (4) loss of strength due to decarburization, (5) loss of ductility from carburization, (6) crack propagation, and (7) loss

of fatigue resistance. Some or all of the above may be important. Very often, the "sodium effects" are difficult to separate from changes in material properties occurring from the long exposure in the temperature range 300^o to 700^oC. This discussion is logically divided into two parts, one dealing with fuel cladding and one dealing with other reactor components, since the sodium effects on cladding are more severe.

Fuel Cladding

In addition to the loss of cross-section from mass loss, allowance must be made for effective loss caused by ferrite layer formation and intergranular penetration. The sum of these effects can be 50 micrometers for one year service at 700^oC. This amount of material represents about 15% of the effective wall thickness of present fuel cladding and must be accounted for in fuel assembly design (similar types of allowances must be made to accomodate interactions between cladding and fuel on the inner diameter of the tube).

Added to the effective loss in section thickness is the possible loss of stress-rupture properties (both time-to-rupture and strain-at-rupture). All annealed and "carbide-agglomerated" 304 and 316 fuel cladding has shown loss of strength from decarburization and sigma phase formation in out-of-reactor tests and 30 to 40% loss in stress-to-rupture after 10,000 hours at 705^oC.⁽⁵⁾ The only measured loss of strength in the FFTF 20% cold worked 316 stainless

steel has been reported by Shively.⁽²⁸⁾ All the above observations were made at 650°C and above; below 620°C, loss of stress-rupture properties in 304 and 316 stainless steel from sodium exposure is hardly noticeable, based upon comparison with control specimens in an argon environment. Loss of stress-rupture properties in stabilized alloys (321, 347, Alloy 800) is expected to be less because of the absence of carbon loss. The effect of sodium exposure on creep and stress-rupture behavior in the advanced candidate cladding materials must be determined. In-reactor experience of 20% cold-worked 316 SS has in general been satisfactory. One test fuel assembly was irradiated in EBR-II in flowing sodium for over 9000 hours at maximum temperatures of 620 to 700°C, with no cladding breaches, excessive deformation or measurable decarburization.⁽¹³⁾

Heat Exchanger and Steam Generator Tubes

Because heat exchanger temperatures are generally lower (550°C and below) than those in the core, and walls are much thicker than cladding, mass loss is not considered important. There is potential loss of carbon in the maximum temperature region of the secondary side of the IHX, (normally constructed of austenitic stainless steel) and also from 2-1/4 Cr - 1 Mo alloy steam generator tubes but the carbon transport rate is likely to be rather slow. The RAPSODIE⁽³⁷⁾ and BOR-60⁽³⁸⁾ intermediate heat exchangers have operated successfully in the 500 to 540°C range, but the units are much smaller (30 MW_{th} or less compared to up to 500 MW_{th} in future breeder reactors) and have operated only six years, compared to 30-year life-

times for breeder plants, hence the long-term effects of sodium environment are not yet available.

Other Components

For other reactor components, the most outstanding effect of the sodium environment is to provide a super-clean environment, as in a vacuum system with a pressure of 10^{-20} Torr or lower (such vacuum systems do not exist except in outer space!). Little change in properties is observed; results of investigations are summarized below:

- 1) Fatigue lifetimes and tensile strengths of 304 and 316 SS sheet and rod increased or were unaffected by sodium exposures at 600 to 700°C.⁽³⁹⁾ The pickup of carbon from test loop sodium was the cause of the increased strength.
- 2) Fatigue cracks in austenitic stainless steel do not propagate more rapidly in sodium than in vacuum or helium.⁽⁴⁰⁾ This fact can be attributed to the lack of "wedging" of an oxide phase at the tip of the crack. This study was limited to pre-cracked specimens, so the effect of sodium exposure on crack initiation has not been determined.
- 3) At temperatures lower than those of the studies in Item 1 above, the carbon pickup is likely to produce a carbide phase near or on

the surface. This phase may be more brittle than the underlying austenitic matrix, but, as mentioned, cracks will not propagate rapidly in the steel. The test loop piping used for some of the cladding stress rupture studies was examined after the tests; 75 to 125 μm deep groves did not propagate as cracks even after 17,600 hours at 700°C.

Carbide Precipitation

The precipitation of carbides in the austenitic stainless steels can affect long-term mechanical properties and swelling resistance of fuel cladding; this effect would occur in any environment. Mass transfer (loss or gain) of the austenitic steels is not noticeably affected by the precipitation. Examination of the regions around weldments in test loops has also shown no unusual effects because of the weldment.

Load Pads and Low-Friction Surfaces

The need for low-friction sliding surfaces exists several places in a reactor. The "load pad" on a fuel duct that enables the fuel assemblies to slide past one another during refueling is an example. Because of the extremely low oxygen activity of sodium, load pad materials that depended on the low-friction coefficient of oxide films failed. Chromium carbide and nickel-aluminide coating materials have been developed which have the necessary sodium compatibility, low-friction behavior, and stability in an irradiation environment. (41,42,43)

CONCLUSIONS

The published reports included in the discussion above show that a great deal is known about the interaction of sodium with the materials and components of liquid-metal-cooled reactors. The transfer of science to technology is rapid. The present generation of sodium-cooled reactors are being built with confidence in the soundness of the sodium systems and a long in-sodium life for components. Materials selection and component design are based on firm, if somewhat conservative, criteria.

Continuing work is needed, however, to refine the technological base in such areas as in-reactor measurement of corrosion, effect of prolonged sodium exposure on mechanical properties of metals, and the chemistry of impurities in sodium. This latter topic includes the measurement and control of interstitial elements and radioactive species.

Sodium is essentially a benign and easily handled heat transfer medium. The science and technology of liquid metal systems had advanced rapidly. Without a doubt the use of liquid metal heat transfer systems in energy conversion systems other than nuclear fission reactors will increase as the success of present systems continues to be demonstrated.

ACKNOWLEDGEMENTS

The author acknowledges the assistance and support of Dr. Robert L. Eichelberger of the Energy Technology Engineering Center (formerly Liquid Metal Engineering Center), Santa Susana, California; who collaborated with the author on a previous review article.⁽⁴³⁾

This work was sponsored by the United States Department of Energy under contract EY-76-C-14-2170.

REFERENCES

1. L. E. Chulos, "Operational Techniques Employed for the Liquid Sodium Source Term Control Loops," paper II-A-8 in Proceedings of International Conference Liquid Metal Technology in Energy Production, Champion, PA, May 1976, CONF-760503. (Ref 25)
2. J. J. McCown and H. C. Duncan "Sodium and Cover Gas Chemistry in the High Temperature Sodium Facility" Paper II-A-5 in Reference 25.
3. D. L. Smith and R. H. Lee, "Characterization of the Vanadium Wire Equilibration Method for Measurement of Oxygen Activity in Liquid Sodium, ANL-7891, January 1972.
4. B. R. Grundy et. al, "Characterization of On-Line Liquid Metal Oxygen Meters, WARD-3045-4 (1972).
5. "Effect of Sodium Exposure on the Corrosion and Strength of Stainless Steels, Summary Report," GEAP-10394 (1971).
6. C. Bagnall and D. C. Jacobs, "Relationships for Corrosion of Type 316 Stainless Steel in Liquid Sodium," WARD-NA-3045-23 (1974).
7. A. W. Thorley and C. Tyzack, "Corrosion Behavior of Steels and Nickel Alloys in High-Temperature Sodium," Paper SM-85/18, Alkali Metal Coolants, Proceedings of International Atomic Energy Agency Symposium, Vienna (1976) (Reference 20).
8. P. Roy and M. K. Schad, J. Nucl. Material, 47 (1973) pp. 129-131.
9. J. R. Weeks, et al, "Corrosion and disposition of steels and Ni-base Alloys in Sodium," BNL-15731 (1971) (also in Ref. 23, pp. 207-214)
10. W. F. Brehm, "Effect of Oxygen in Sodium Upon Radionuclide Release from Austenitic Stainless Steel," HEDL-SA-985 (1975). Presented at IAEA Specialists' Meeting on Fission and Corrosion Products in Primary Systems of LMFBR's, Dimitrovgrad, USSR, Sept. 1975, IWGFR-7.
11. W. F. Brehm, "Radioactive Corrosion Product Transport and Control," Paper IV-B-1 in Reference 25.
12. M. C. Rowland et al, "Behavior of Selected Steels Exposed in Flowing Sodium Test Loops," GEAP-4831 (1965).
13. J. W. Weber, "In-reactor Corrosion Behavior of Stainless Steel in High-Temperature Sodium," Paper V-B-3 in Reference 25.
14. J. Hopenfeld, "Corrosion of Type 316 Stainless Steel with Surface Heat Flux in 1200°F Flowing Sodium," AI-AEC-12898 (1969).

31. R. P. Colburn, "Characterization of Corrosion Product Deposits in Sodium Systems" HEDL-SA-1452, Presented at IAEA Specialists Meeting on Sodium Removal and Decontamination, Richland, Washington, February 1978.
32. W. E. Ray et al., "The Structure and Properties of Sodium Mass Transfer Deposits," Paper IV-1 at ANS Topical Meeting on Reactor Materials Performance, Richland, Washington, April 1972.
33. W. H. Yunker, "Formation and Hydraulic Effects of Deposits in High Temperature Sodium Coolant Systems," Paper VII-B-2 in Reference 25.
34. A. A. Bishop et al, "Mass Transfer Related Pressure Drop Fluctuations in Flowing Sodium Systems," Paper VII-B-3 in Reference 25.
35. J. C. McGuire and W. F. Brehm, "Progress in Radionuclide Trap Development," HEDL-TME 77-85 (1978).
36. J. C. Clifford et al, "Behavior of Fission Products in Sodium," Paper SM-85/30 in Reference 20.
37. V. I. Polyakov et al, "Radioactive Product Behavior During the Operation of Sodium-Cooled Reactors of the U.S.S.R.," Paper I-4 in Reference 25.
38. R. de Fremont, "Observations on the Behavior of Radioactive Products on RAPSODIE," IAEA Specialists' Meeting on Fission and Corrosion Products in Primary Systems of LMFBR's, Bensberg, Germany, September 1971, CONF-710959.
39. K. Natesan et al, "Effect of Sodium on the Creep-Rupture Behavior of Type 304 Stainless Steel," Paper V A-4 in Reference 25.
40. L. A. James and R. L. Knecht, "Fatigue Crack Propagation Behavior of Type 304 Stainless Steel in a Liquid Sodium Environment," Met. Trans. 6A, 109-116 (1975).
41. R. N. Johnson et al, "Development of Low Friction Materials for LMFBR Components," Paper II B-1 in Reference 25.
42. G. A. Whitlow et al, "Corrosion and Tribological Investigations of Chromium Carbide Coatings for Sodium Cooled Reactor Applications," Paper II-B-3 in Reference 25.
43. N. J. Hoffman et al, "Evaluation of Cobalt and Nickel Base Materials for Sliding and Static Contact Applications in a Liquid Metal Fast Breeder Reactor," Paper II-B-7 in Reference 25.
44. W. F. Brehm and R. L. Eichelberger, "Effects of Sodium Environment on Breeder Reactor Components," HEDL-SA-1420. Preprint #106 at National Association of Corrosion Engineers (NACE) Meeting; Houston, Texas, March 1978.